



Representation of spatial and temporal variability in large-domain hydrological models: case study for a mesoscale pre-Alpine basin

Lieke Melsen¹, Adriaan Teuling¹, Paul Torfs¹, Massimiliano Zappa², Naoki Mizukami³, Martyn Clark³, and Remko Uijlenhoet¹

¹Hydrology and Quantitative Water Management Group, Wageningen University, Wageningen, the Netherlands

²Swiss Federal Research Institute (WSL), Birmensdorf, Switzerland

³National Center for Atmospheric Research (NCAR), Boulder, CO, USA

Correspondence to: Lieke Melsen (lieke.melsen@wur.nl)

Received: 10 December 2015 – Published in Hydrol. Earth Syst. Sci. Discuss.: 27 January 2016

Revised: 25 May 2016 – Accepted: 25 May 2016 – Published: 8 June 2016

Abstract. The transfer of parameter sets over different temporal and spatial resolutions is common practice in many large-domain hydrological modelling studies. The degree to which parameters are transferable across temporal and spatial resolutions is an indicator of how well spatial and temporal variability is represented in the models. A large degree of transferability may well indicate a poor representation of such variability in the employed models. To investigate parameter transferability over resolution in time and space we have set up a study in which the Variable Infiltration Capacity (VIC) model for the Thur basin in Switzerland was run with four different spatial resolutions (1 km × 1 km, 5 km × 5 km, 10 km × 10 km, lumped) and evaluated for three relevant temporal resolutions (hour, day, month), both applied with uniform and distributed forcing. The model was run 3150 times using the Hierarchical Latin Hypercube Sample and the best 1 % of the runs was selected as behavioural. The overlap in behavioural sets for different spatial and temporal resolutions was used as an indicator of parameter transferability. A key result from this study is that the overlap in parameter sets for different spatial resolutions was much larger than for different temporal resolutions, also when the forcing was applied in a distributed fashion. This result suggests that it is easier to transfer parameters across different spatial resolutions than across different temporal resolutions. However, the result also indicates a substantial underestimation in the spatial variability represented in the hydrological simulations, suggesting that the high spatial transferability may occur because the current generation of large-domain

models has an inadequate representation of spatial variability and hydrologic connectivity. The results presented in this paper provide a strong motivation to further investigate and substantially improve the representation of spatial and temporal variability in large-domain hydrological models.

1 Introduction

The history of modern hydrological modelling dates back to halfway through the nineteenth century, starting with empirical models to predict peak flows (Todini, 2007). For a long time, hydrological models were developed only at the catchment scale, evolving from empirically based to more physically based. Computational power and increased data availability have driven the development of increasingly complex and distributed hydrological models (Boyle et al., 2001; Liu and Gupta, 2007). Distributed hydrological models can incorporate spatially varying parameters, including those reflecting land use and soil characteristics (Carpenter and Georgakakos, 2006), and spatially variable forcing. In 1989 the first global hydrological model (GHM) was presented (Vörösmarty et al., 1989; Sood and Smakhtin, 2015). Continuing improvements in computational power and data availability provide new opportunities for GHMs, for example expressed in the recent ambition to develop global models with a resolution of the order of ~ 1 km and higher, the so-called hyper-resolution (Wood et al., 2011; Bierkens et al., 2014; Bierkens, 2015).

Because the parameters in hydrological models often represent a different spatial scale than the observation scale, or because conceptual parameters have no directly measurable physical meaning, calibration of hydrological models is almost always inevitable (Beven, 2012). The increased complexity of hydrological models and the increased application domain has resulted in more complex and time consuming optimization procedures for the model parameters. However, although recent developments in e.g. satellites and remote sensing can provide spatially distributed data to construct and force models, discharge measurements are still required to calibrate and validate model output.

Both to decrease calculation time of the optimization procedure and to be able to apply the model in ungauged or poorly gauged basins and areas, many studies have focused on the transferability of parameter values over time, space, and spatial and temporal resolution (e.g. Wagener and Wheeler, 2006; Duan et al., 2006; Troy et al., 2008; Samaniego et al., 2010; Rosero et al., 2010; Kumar et al., 2013; Bennett et al., 2016). Sometimes it is assumed that parameters are directly transferable, for example by calibrating on a coarser time step than the time step at which the model output will eventually be analysed (e.g. Liu et al., 2013; Costa-Cabral et al., 2013). Troy et al. (2008) rightly question what the effect is of calibrating at one time step and transferring the parameters to another time step. Their results suggest that the time step had only limited impact on the calibrated parameters and thus on the monthly runoff ratio. On the other hand, Haddeland et al. (2006) found that modelled moisture fluxes are sensitive to the model time step. Several studies (e.g. Littlewood and Croke, 2008, 2013; Kavetski et al., 2011 and Wang et al., 2009) have found that parameter values are closely related to the employed time step of the model. Chaney et al. (2015) investigated to what extent monthly runoff observations could reduce the uncertainty around the flow duration curve of daily modelled runoff. They found a decrease in the uncertainty around the flow duration curve when the monthly discharge observations were used, but the magnitude of the reduction was dependent on climate type. Recently, Ficchi et al. (2016) conducted a thorough analysis of the effect of temporal resolution on the projection of flood events, where it was shown that the flood characteristics determined the sensitivity for the temporal resolution.

Less intuitive and less common is to transfer parameters across different grid resolutions. Haddeland et al. (2002) showed that the output of the Variable Infiltration Capacity (VIC) model was significantly different when the parameters of the model were kept constant for several spatial resolutions. For the same model, Liang et al. (2004) showed that model parameters calibrated at a coarse grid resolution could be applied to finer resolutions to obtain comparable results. Troy et al. (2008), on the contrary, found that calibrating the VIC model on a coarse resolution significantly affected the model performance when applied to finer resolutions. Finnerty et al. (1997) investigated parameter transfer-

ability over both space and time for the Sacramento model, and showed that it can lead to considerable volume errors.

Although the ambition of GHMs is to move towards hyper-resolution (~ 1 km and higher), more physically based catchment models have already been applied at spatial resolutions of the order of 100 m. Also for these models at this scale, the effect of spatial resolution has been investigated (e.g. Vivoni et al., 2005; Sulis et al., 2011; Shrestha et al., 2015). Even for fully coupled surface-groundwater land-surface models, the effect of spatial resolution on hydrologic fluxes was found to be considerable (Shrestha et al., 2015).

The impact of transferring parameters across spatial and/or temporal resolutions on model performance is thus ambiguous, but relevant in the light of hydrological model development, especially for GHMs which are at the upper boundary of computational power and data availability. Calibration on a coarse temporal or spatial resolution and subsequently transferring to a higher resolution could potentially reduce computation time, and it is therefore relevant to investigate the opportunities. But parameter transferability across spatial and temporal resolutions is also interesting for another reason: it is an indicator of the degree to which spatial variability and temporal variability are represented in the model. Ideally, in a model that describes all relevant hydrological processes correctly, parameters should to a large extent be transferable over time because longer time steps are simply an integration of the shorter time steps. On the other hand, parameters should not be or be hardly transferable over space, because the physical characteristics which they represent are different from place to place. Investigating parameter transferability across spatial and temporal resolutions can thus provide insight into the model's representation of spatial and temporal variability.

In this study, we employ the Variable Infiltration Capacity (VIC) model (Liang et al., 1994), which has also been applied at the global scale (Nijssen et al., 2001; Bierkens et al., 2014), to study parameter transferability across temporal and spatial resolutions, accounting for the difference between uniform and distributed forcing. We applied this study to a well-gauged meso-scale catchment in Switzerland (the Thur basin, 1703 km²) on spatial resolutions that are relevant for hyper-resolution studies (1 km \times 1 km, 5 km \times 5 km and 10 km \times 10 km, as well as a lumped model which represents the 0.5° grid used in many global studies). We use the most common temporal resolutions for which discharge data are available (hourly, daily, monthly). We ran the models both with distributed forcing (different forcing input for each grid cell) and with uniform forcing (same forcing input for each grid cell), where the latter is in line with many of the data sets currently used for forcing global hydrological models (e.g. WATCH forcing data, 0.5°).

Several studies already investigated scale effects in the VIC model, for instance Haddeland et al. (2002, 2006), Liang et al. (2004), Troy et al. (2008), Wenger et al. (2010) and Wen et al. (2012). This study is novel in that we choose a

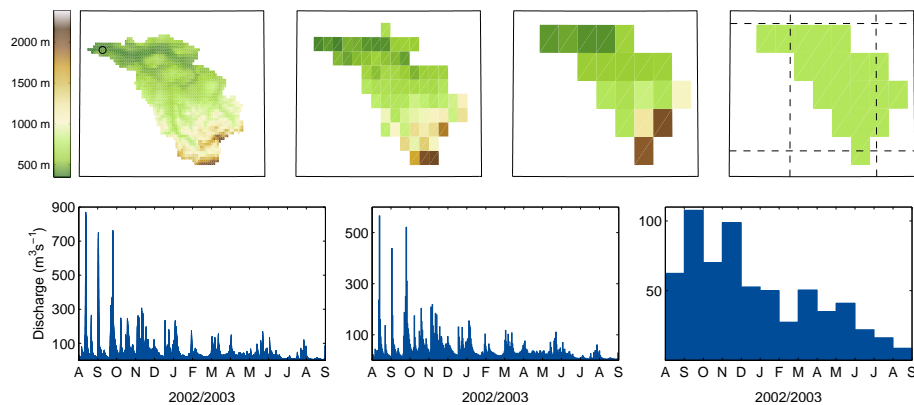


Figure 1. Overview of the spatial and temporal resolutions employed in this study. Top panels from left to right: DEM (digital elevation model) grid cells for 1 km × 1 km, 5 km × 5 km, 10 km × 10 km resolution and the lumped model. The circle in the left panel shows the location of the Thur outlet where the discharge is measured. The dotted lines in the right panel indicate a 0.5° grid. Bottom panels: the three temporal resolutions; observed discharge at an hourly, daily and monthly time step.

probabilistic approach rather than a deterministic approach: essentially we employ a GLUE-based approach (Beven and Binley, 1992, 2014) in which we implicitly account for parameter uncertainty. We quantify parameter transferability by evaluating the overlap in behavioural sets for different temporal and spatial resolutions. To determine the behavioural sets, we make use of three different objective functions focusing on high flows, average conditions, and low flows. It is also novel that we test the effect of forcing on the results, and that we use several subbasins to explain the results. Our case study provides a benchmark for parameter transferability for models applied at larger scales, dealing with the same spatial and temporal resolutions as employed here. The results of our study also provide an indication of the current status of spatial and temporal representation in the VIC model, being representative of a larger group of land-surface models.

2 Catchment and data description

2.1 Thur basin

The Thur basin (1703 km²; see Figs. 1 and 2) in north-eastern Switzerland was chosen as the study area, because of the excellent data availability in this area and because of its relevance as a tributary of the river Rhine (Hurkmans et al., 2008). The main river in the basin (the Thur) has a length of 127 km. The average elevation of the basin is 765 m a.s.l., and the mean slope is 7.9° (based on a 200 m × 200 m resolution DEM and slope file). The basin outlet is situated at Andelfingen at an elevation of 356 m a.s.l. (Gurtz et al., 1999). The basin has an Alpine/pre-Alpine climatic regime, with high temperature variations both in space and time (Fig. 3). Precipitation varies from 2500 mm yr⁻¹ in the mountains to 1000 mm yr⁻¹ in the lower areas. Part of the year the basin is covered with snow. The most striking feature in the

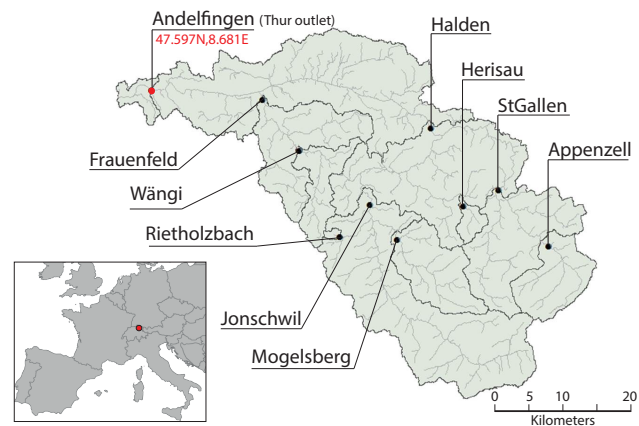


Figure 2. The Thur basin and the nine sub-basins for which discharge data were available.

Thur basin is the Säntis, an Alpine peak with an altitude of 2502 m. The dominant land use in the Thur basin is pasture. Within the Thur basin, measurements for nine (nested) sub-catchments are available (see Fig. 2). The smallest gauged sub-catchment is the Rietholzbach catchment (3.3 km²; see Seneviratne et al., 2012); the largest is Halden (1085 km²). Both the Rietholzbach and the Thur have been the subject of many previous studies (e.g. Gurtz et al., 1999, 2003; Jasper et al., 2004; Abbaspour et al., 2007; Yang et al., 2007; Teuling et al., 2010; Melsen et al., 2014). In this study, we will mainly focus on the outlet of the Thur basin.

2.2 Discharge data

For the station at the Thur outlet (Andelfingen) and eight sub-basins, hourly discharge measurements for the period 1974–2012 were made available by the Swiss Federal Office for the Environment (FOEN). All discharge measurements have

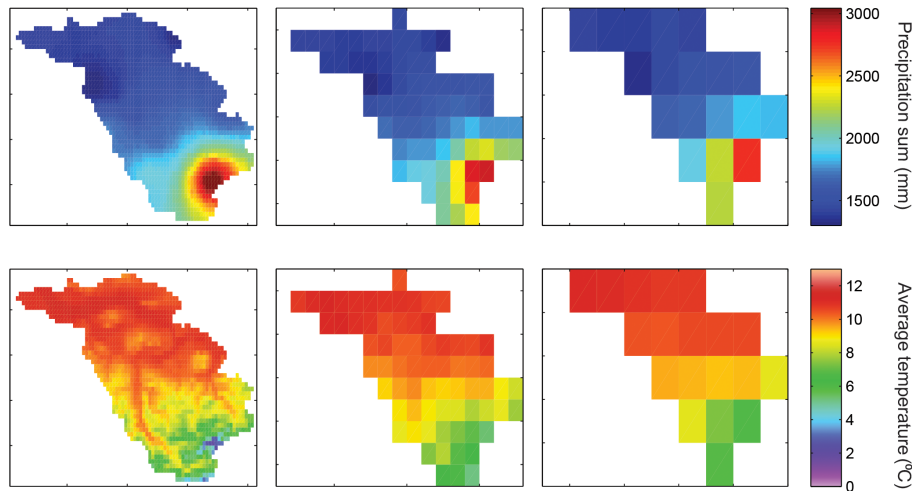


Figure 3. Upper panels: the precipitation sum in the Thur catchment over the full model period (1 August 2002–31 August 2003) shown for different resolutions (f.l.t.r.: 1 km \times 1 km, 5 km \times 5 km, 10 km \times 10 km). Lower panels: the average temperature over this period for the same spatial resolutions.

been obtained using a stage–discharge relation, based on several measurements conducted by FOEN throughout the years, amongst others, with an ADCP. The discharge measurements for the Rietholzbach catchment were made available by ETH Zürich.

2.3 Forcing data

Forcing data for this study were made available by the Swiss Federal Office for Meteorology and Climatology (MeteoSwiss). These data have previously been used for numerous applications of hydrological models in the Thur (Jasper et al., 2004; Abbaspour et al., 2007; Fundel and Zappa, 2011; Fundel et al., 2013; Jörg-Hess et al., 2015). The data are available for this study in the form required to implement the PREVAH model (Viviroli et al., 2009a, b). Data from nine different meteorological stations throughout the catchment (Güttingen, Hörnli, Reckenholz, Säntis, St. Gallen, Tänikon, Wädenswil, Zürich and Rietholzbach) were available with an hourly time resolution and spatially interpolated with the use of the WINMET tool of the PREVAH modelling system (Viviroli et al., 2009a), using elevation-dependent regression (EDR) and inverse distance weighting (IDW) and combinations of IDW and EDR. The data are available for the period 1981–2004, for which a stable configuration of stations is available. In this study, we only used data for the period May 2002–August 2003. To force the VIC model, hourly precipitation, incoming shortwave radiation, temperature, vapour pressure and wind data were used. We have run the model with two set-ups: fed with uniform forcing and fed with distributed forcing. Because the Thur basin has an extent of approximately 0.5° , a lumped application of the forcing mimics the use of global forcing data sets like the WATCH forcing product and the ERA-Interim product. Ap-

plication with distributed forcing implied different forcing inputs for each grid cell. Because of the pronounced elevation differences in the basin, precipitation and temperature show a clear spatial pattern, which can be seen in Fig. 3.

2.4 Spatial data for the model

Land use, hydraulic conductivity, elevation, and soil water storage capacity maps, all with a spatial resolution of 200 m \times 200 m, were provided by the Swiss Federal Institute for Forest, Snow and Landscape Research (WSL) under license by swisstopo (JA100118). Also in this case we used the pre-processing routines created to implement the PREVAH modelling system (Viviroli et al., 2009a). The resolution of the available data (200 m \times 200 m) is higher than the model with the highest resolution in this study (1 km \times 1 km), which allows for sub-grid variability in the VIC model for land use and elevation parameters (see Sect. 3.1). Other soil characteristics, such as bulk density, have been obtained from the Harmonized World Soil Database (FAO et al., 2012), which has a spatial resolution of 1 km \times 1 km.

3 Model and routing description

The VIC model (version 4.1.2.i) was run at an hourly time step in the energy balance mode, which implies that both the water and energy balances are solved. The default routing developed for VIC by Lohmann et al. (1996) is only applicable at daily time steps and hence is not suitable for studying parameter transferability at finer temporal resolutions. Therefore, horizontal water transport through the channel network was implemented using mizuRoute (Mizukami et al., 2015).

3.1 The VIC model

The VIC model (Liang et al., 1994, 1996) is a land-surface model that solves the water and the energy balance. Subgrid land-use type variability is accounted for by providing vegetation tiles that each cover a certain percentage of the total surface area. Three different types of evaporation are considered by the VIC model: evaporation from the bare soil (E_b), transpiration by the vegetation (T), considered per vegetation tile, and evaporation from interception (E_i). The total evapotranspiration is the area-weighted sum of the three evaporation types. The fraction of land that is not assigned to a particular land-use type is considered to be bare soil. Evaporation from bare soil only occurs at the top layer (layer 1). If layer 1 is saturated, bare soil evaporation is at its potential rate. Potential evaporation is obtained with the Penman–Monteith equation. If the top layer is not saturated, an Arno formulation (Francini and Pacciani, 1991), which uses the structure of the Xinanjiang model (Zhao et al., 1980), is used to reduce the evaporation.

For the upper two soil layers, the Xinanjiang formulation (Zhao et al., 1980) is used to describe infiltration. This formulation assumes that the infiltration capacity varies within an area. Surface runoff occurs when precipitation added to the soil moisture of layers 1 and 2 exceeds the local infiltration capacity of the soil. Moisture transport from layer 1 to layer 2 and from layer 2 to layer 3 is gravity driven and only dictated by the moisture level of the upper layer. It is assumed that there is no diffusion between the different layers. Layer 3 characterizes long-term soil moisture response, e.g. seasonality. It only responds to short-term rainfall when both top layers are fully saturated. The gravity-driven moisture movement is regulated by the Brooks–Corey relationship:

$$Q_{i,i+1} = K_{\text{sat},i} \left(\frac{W_i - W_{r,i}}{W_i^c - W_{r,i}} \right)^{\text{exp}t_i} \quad (1)$$

$Q_{i,i+1}$ is the flow [$\text{L}^3 \text{T}^{-1}$] from layer i to layer $i+1$. $K_{\text{sat},i}$ is the saturated hydraulic conductivity of layer i , W_i is the soil moisture content in layer i , W_i^c is the maximum soil moisture content in layer i , and $W_{r,i}$ the residual moisture content in layer i . The exponent of the Brooks–Corey relation, $\text{exp}t_i$, is defined as follows: $\frac{2}{B_p} + 3$, in which B_p is the pore size distribution index. The exponent as a whole is often calibrated.

Baseflow is determined based on the moisture level of layer 3. Baseflow generation follows the conceptualization of the Arno model (Francini and Pacciani, 1991). This formulation consists of a linear part (lower moisture content regions) and a quadratic part (in the higher moisture regions). Baseflow is modelled as follows:

$$Q_b = \begin{cases} \frac{d_s d_m}{w_s W_3^c} \cdot W_3 & \text{if } 0 \leq W_3 \leq w_s W_3^c \\ \frac{d_s d_m}{w_s W_3^c} \cdot W_3 + \left(d_m - \frac{d_s d_m}{w_s} \right) \left(\frac{W_3 - w_s W_3^c}{W_3^c - w_s W_3^c} \right)^g & \text{if } W_3 \geq w_s W_3^c \end{cases}$$

In this equation, Q_b is the total baseflow over the model time step (in this study, 1 h), d_m is the maximum baseflow, d_s is the fraction of d_m where non-linear baseflow begins, and w_s is the fraction of soil moisture where non-linear baseflow starts. W_3^c is the maximum soil moisture content in layer 3, calculated as a product of porosity and depth. The exponent g is by default set to 2 (Liang et al., 1996).

Since the grid size of the VIC model is often larger than the characteristic scale of snow processes, sub-grid variability is accounted for by means of elevation bands. For each grid cell the percentage of area within certain altitude ranges is provided. The snow model is applied for each elevation band and land-use type separately; the weighted average provides the output per grid cell. This output consists of the snow water equivalent (SWE) and the snow depth. The snow model is a two-layer accumulation–ablation model, which solves both the energy and the mass balance. At the top layer of the snow cover the energy exchange takes place. A zero energy flux boundary is assumed at the snow–ground interface. A complete description of the model can be found in Liang et al. (1994, 1996).

3.2 Routing

The mizuRoute routine (Mizukami et al., 2015) takes care of the transport of water between the different grid cells. The routing is based on the same concept as the routing described by Lohmann et al. (1996), except that in mizuRoute the response is determined per subcatchment instead of per grid cell.

With the linearized St. Venant equation,

$$\frac{\partial Q}{\partial t} = D \frac{\partial^2 Q}{\partial x^2} - C \frac{\partial Q}{\partial x} \quad (2)$$

water is transported from the boundary of the subcatchment to the next subcatchment and finally to the outlet. In Eq. (2), D ($\text{m}^2 \text{s}^{-1}$) represents the diffusion coefficient and C (m s^{-1}) the advection coefficient.

In the Thur basin, the routing is applied to subcatchments of the order of 1 km^2 . It is important to note that with the applied routing set-up, the drainage network is kept independent of the resolution, because surface runoff is routed for pre-defined sub-basins instead of per grid cell. In the default VIC routing of Lohmann et al. (1996), water is routed per grid cell and is therefore dependent on the spatial resolution of the VIC model. By applying mizuRoute based on pre-defined sub-basins ($\sim 1 \text{ km}^2$), we have excluded the effect of the spatial resolution on the routing process.

4 Experimental set-up

We have constructed four VIC models with different spatial resolutions: $1 \text{ km} \times 1 \text{ km}$, $5 \text{ km} \times 5 \text{ km}$, $10 \text{ km} \times 10 \text{ km}$, as well as a lumped model. These models have been run with

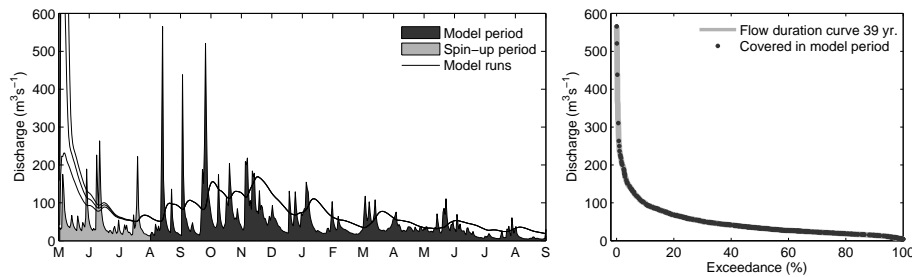


Figure 4. Daily discharge characteristics for the Thur basin. Left panel: the daily discharge in the Thur for the selected model period. The black lines show three model runs with the same parameter set but with different initial conditions ($\theta = 0.5, 0.7, 0.9$). Right panel: part of the flow duration curve covered within the model period. The flow duration curve is based on 39 years of daily discharge observations in the Thur basin for the period 1974–2012.

both uniform and distributed forcing. Since for the lumped model there is no difference between uniform and distributed forcing, this leads to a total of seven different model setups. Because the runtime of the model combined with all the post-processing is rather long (on average 2.5 h for the $1 \text{ km} \times 1 \text{ km}$ model on a standard PC), an efficient sampling strategy was designed. The procedure we followed is illustrated in Fig. 5. With sensitivity analysis (Sect. 4.4) the most sensitive parameters from the model were selected. Subsequently, we sampled the full parameter space with a uniform prior using the Hierarchical Latin Hypercube Sample (HLHS) (Vorˆechovskˆy, 2015); see Sect. 4.5. Although sampling the parameter space with a uniform prior is less efficient than other distributions which focus more on the most likely regions, we did not want to exclude any region because both the temporal and spatial resolution were varied. The sampled parameters were applied uniformly over the catchment, whereas all other soil- and land-use parameters have been applied in a distributed fashion. After running the models with the HLHS, the output was evaluated and the best 1 % of the runs was defined as behavioural. The overlap in behavioural sets was used as an indicator of parameter transferability (Sect. 4.7).

4.1 Spatial model resolution

Four VIC implementations with different spatial resolutions (0.0109° roughly corresponding to $1 \text{ km} \times 1 \text{ km}$, $0.0558^\circ \approx 5 \text{ km} \times 5 \text{ km}$, $0.1100^\circ \approx 10 \text{ km} \times 10 \text{ km}$, as well as a lumped model) were constructed. The $1 \text{ km} \times 1 \text{ km}$ model represents the so-called hyper-resolution. Several studies already explore GHMs at this resolution, e.g. Sultanudjaja et al. (2014) for the Rhine–Meuse basin. The model with the $10 \text{ km} \times 10 \text{ km}$ resolution can be characterized as “regional”. The $5 \text{ km} \times 5 \text{ km}$ model is in between the hyper-resolution scale and the regional scale. The lumped model, which represents an area of 1703 km^2 , is of the order of magnitude of grid cells with a 0.5° resolution, which represents the original scale for which VIC was developed. Figure 1 gives an overview of the cell size of the four models. The

sampled parameters (see Sect. 4.4) have been applied uniformly over the catchment; all other parameters have been applied in a distributed manner. We will discuss the effect of applying the sampled parameters uniformly by using data from the nine subcatchments.

4.2 Temporal model resolution

The models are run at an hourly time step, implying that they solve both the energy and the water balance. The hourly output of the routing model is aggregated to daily and monthly time steps for further evaluation; see Fig. 1.

4.3 Simulation period

The four models are run for a period of 1 year and 4 months. The first 3 months are used as a spin-up period and are not used for further analysis. Tests with the same parameter set and different initial conditions revealed that 3 months are sufficient to eliminate the effect of initial conditions (see Fig. 4). The initial soil moisture content of the model before spin-up was fixed at $\theta = 0.9$ because we found that the model reaches equilibrium faster when starting from a wet state. The models have not been subjected to a validation procedure on another time period, because in this particular application the goal was not to identify the best performing model, but to investigate the role of temporal and spatial resolution in parameter transferability.

The analysed period is 1 August 2002–31 August 2003 (see Fig. 4). This period is characterized by three very high peaks (August, September 2002) as well as the severe 2003 drought (June, July, August 2003). The 2002 peaks (see e.g. Schmocker-Fackel and Naef, 2010) have an estimated return period of 15 to 20 years. The peaks were caused by a larger system that also caused the heavy floods in the Elbe and the Danube (Becker and Gr̈unewald, 2003). In contrast, the 2003 summer was extremely warm and dry in western and central Europe (Miralles et al., 2014), with Switzerland being among the hottest and driest regions (Andersen et al., 2005; Rebetez et al., 2006; Zappa and Kan, 2007; Senevi-

Table 1. Sampled model parameters.

Parameter	Units	Lower value	Upper value	Description
b_i	–	10^{-5}	0.4	Variable infiltration curve parameter
d_s	–	10^{-4}	1.0	Fraction of $d_{s,max}$ where non-linear baseflow starts
d_m	mm day ⁻¹	1.0	50	Maximum velocity of the baseflow
expt ₂	–	4.0	18.0	Exponent of the Brooks–Corey drainage equation for layer 2
Depth ₂	m	Depth ₁ + 0.1	Depth ₁ + 3	Depth of soil layer 2
C	ms ⁻¹	0.5	4	Advection coefficient of horizontal routing (St. Venant)
D	m ² s ⁻¹	200	4000	Diffusion coefficient of horizontal routing (St. Venant)

ratne et al., 2012). With these two extremes the selected period covers a large part of the flow duration curve, in both the high and low flow regions (right panel in Fig. 4).

4.4 Model parameters

The VIC model has a large number of parameters, divided over three sections: soil parameters, vegetation parameters, and snow parameters. To determine which parameters should be sampled in this study, a sensitivity analysis was conducted on a broad selection of parameters (see Table S1 in the Supplement). The parameter selection was made such that the main hydrological processes were represented and included 28 VIC parameters from the three different sections. Sensitivity analysis was conducted using the distributed evaluation of local sensitivity analysis (DELSA) method (Rakovec et al., 2014). DELSA is a hybrid local–global sensitivity analysis method. It evaluates parameter sensitivity based on the gradients of the objective function for each individual parameter at several points throughout the parameter space. Note that this method only provides first-order sensitivities and thus does not account for parameter interaction.

A base set of 100 parameter samples was created. For each parameter k that is accounted for in the analysis, the base set of parameter samples is perturbed. In total, including the base set, this leads to (number of parameters + 1) × 100 parameter samples that need to be evaluated. To save computation time, the sensitivity analysis was conducted on the lumped VIC model for the Thur basin. To study the effect of spatial scale on sensitivity, two lumped models for subbasins of the Thur have been constructed: the Jonschwil catchment (495 km²) and the Rietholzbach catchment (3.3 km²). The Rietholzbach catchment is nested inside the Jonschwil catchment, which is again nested in the Thur catchment (Fig. 2). The three catchments have comparable land use. The Kling–Gupta efficiency of the discharge (KGE(Q)), Nash–Sutcliffe efficiency of the discharge (NSE(Q)) and the Nash–Sutcliffe efficiency of the logarithm of the discharge (NSE(log Q)) (see Sect. 4.6) were used as objective functions to assess the sensitivity of the parameters.

The analysis showed that parameter sensitivity did not notably change over the assessed scales: the same parameters

were found to be most sensitive, but in a slightly different order (see Fig. S1 in the Supplement). There are four parameters which, for all scales and for all objective functions, proved to be highly sensitive: the parameter describing variable infiltration (b_i), the parameter that defines the fraction of $d_{s,max}$ where non-linear baseflow starts (d_s), the maximum velocity of the baseflow (d_m) and the exponent of the Brooks–Corey relation ($\frac{2}{B_p} + 3$, expt₂; see Eq. 1). Hence, these four parameters were selected for the sampling analysis. Other parameters that showed sensitivity in some cases were the depth and bulk density of soil layer 2, the depth and bulk density of soil layer 3, and the rooting depth of layer 1. The selection of sensitive parameters closely resembles the results of Demaria et al. (2007), who applied a sensitivity analysis to VIC over different hydroclimatological regimes. Because Demaria et al. (2007) found that the depth of soil layer 2 was highly sensitive, this parameter was added to the selection of parameters that was sampled. In addition, the two routing parameters C and D were sampled because they control the lateral exchange of water between grid cells. An overview of the selected parameters is given in Table 1. Because sampling the seven selected parameters in a distributed fashion is computationally extremely demanding and currently not yet feasible, the sampled parameters have been applied uniformly over the cells in the distributed VIC models. This is according to current practice in large-scale modelling.

4.5 Hierarchical Latin Hypercube Sample

In comparison with traditional sampling methods, the number of parameter samples needed to cover the full parameter space can decrease significantly by selecting only the most sensitive parameters (see Fig. 5b). For the four VIC models (three distributed models, one lumped model) the selected parameters (Table 1) were varied using a Latin hypercube sample (LHS). This is a variance reduction method which efficiently samples the parameters within each region with equal probability in the parameter distribution (Vor'echovský and Novák, 2009) (see Fig. 5c). Especially for the 1 km × 1 km model the calculation time is rather long. Therefore, the LHS should preferably be as small as possible,

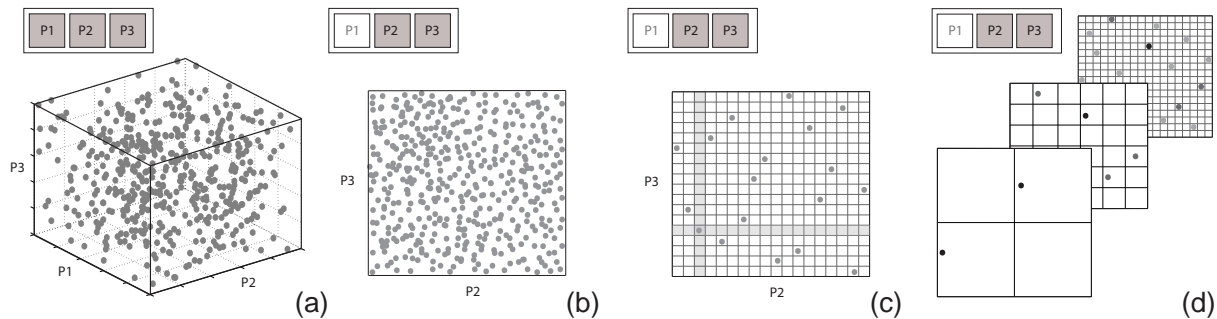


Figure 5. Parameter sampling as applied in this study. **(a)** Example situation when sampling for a model with three parameters. **(b)** Sensitivity analysis can be conducted to decrease the dimensions of the sampling space. **(c)** Latin Hypercube sampling is structured and more efficient: one sample in each row and each column, as indicated with the bands. The number of samples has to be determined beforehand. **(d)** Hierarchical Latin Hypercube Sampling allows to extend the sample if necessary, while conserving Latin hypercube structure.

while still being able to provide insights into e.g. posterior parameter distributions. For a Monte Carlo (MC) sample, it is easy to start with a small sample, and add more samples if this proves to be necessary, e.g. based on the sample variance. For a variance reduction technique such as LHS this is not that straightforward. Therefore, we make use of the Hierarchical Latin Hypercube Sample (HLHS), recently developed by Vorčechovský (2015). This method allows us to start with a small LHS and add more samples if necessary, while conserving the LHS structure (Fig. 5d). Inherent to this method is that every sample extension is twice as large as the previous sample, which results in a total number of simulations after r extensions:

$$N_{\text{sim},r} = 3^r \cdot N_{\text{start}}, \quad (3)$$

with N_{sim} being the total number of simulations, r the number of extensions, and N_{start} the start number of samples. As a starting sample size, 350 is chosen, which is sampled based on a space-filling criterion. For the seven parameters in the HLHS a uniform prior is assumed in order the study the full parameter space. The starting sample can be increased by a first extension to 1050 samples in total, further to 3150, and even up to 9450. After each extension, the cumulative distribution function (CDF) of the objective functions (KGE, NSE) is compared with the CDF of the previous extension. A Kolmogorov–Smirnov test is used to test whether the CDFs are significantly different. It was found that the CDF estimated from 3150 samples was not significantly different from the CDF based on 1050 samples at a 0.05 significance level. Therefore, 3150 samples were considered sufficient to sample the parameter space.

4.6 Objective functions

For each model run, several objective functions were evaluated. The three objective functions are

- the Kling–Gupta efficiency (KGE) to describe the overall capability of the model to simulate the discharge

(Gupta et al., 2009):

$$\text{KGE}(Q) = 1 - \sqrt{(r-1)^2 + (\alpha-1)^2 + (\beta-1)^2}, \quad (4)$$

where r is the correlation between observed discharge Q_o and modelled discharge Q_m , α is the standard deviation of Q_m divided by the standard deviation of Q_o , and β is the mean of Q_m (\bar{Q}_m) divided by the mean of Q_o (\bar{Q}_o);

- the Nash–Sutcliffe efficiency (NSE) of the discharge to describe the model performance for the higher discharge regions (Nash and Sutcliffe, 1970):

$$\text{NSE}(Q) = 1 - \frac{\sum_{t=1}^T (Q_o^t - Q_m^t)^2}{\sum_{t=1}^T (Q_o^t - \bar{Q}_o)^2} = 2 \cdot \alpha \cdot r - \alpha^2 - \beta_n^2, \quad (5)$$

in which β_n is the bias normalized by the standard deviation; and

- the Nash–Sutcliffe efficiency of the logarithm of the discharge $\text{NSE}(\log Q)$ to test the model performance for low discharges (Krause et al., 2005).

The objective functions are calculated for all runs (3150) for the seven different VIC set-ups and based on hourly, daily and monthly time steps.

4.7 Determination of behavioural sets and parameter transferability

After running the VIC model with 3150 parameter sets, a selection is made of the best parameter sets, the so-called behavioural runs (Beven and Binley, 1992). The best 1% (which is different for different objective functions) of the 3150 runs (32 members) are selected as behavioural. For each combination of spatial and temporal resolution, and for

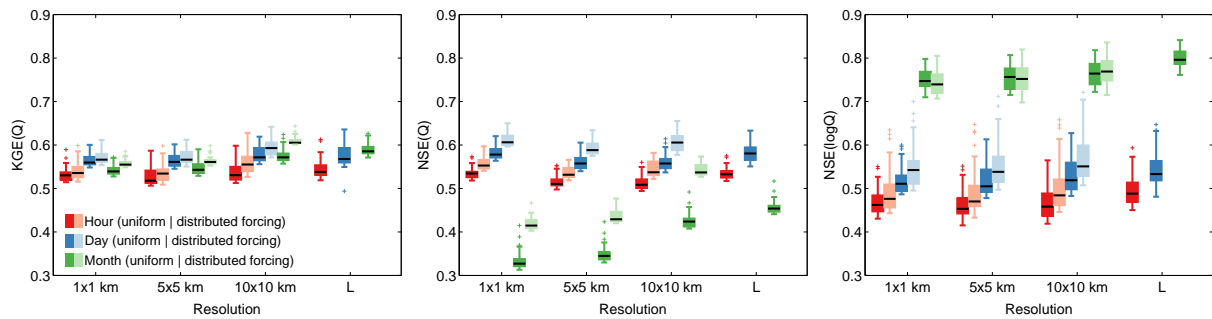


Figure 6. Model performance of the behavioural sets for different temporal resolutions and different spatial resolutions. The left panel shows the $KGE(Q)$, the middle panel the $NSE(Q)$ and the right panel the $NSE(\log Q)$. Per objective function the most behavioural sets were selected; hence, the selected sets were not necessarily the same for the three objective functions. The box shows the 25th–75th percentiles.

the three objective functions separately, the 32 best members are selected. We evaluate all 32 parameter sets as being equally plausible and do not assign weights to the best performing sets within the behavioural selection, to account for uncertainty in the observations. Inherent to our approach, selecting a certain percentage of runs rather than applying a threshold level based on an objective function, is that the selected runs do not necessarily comply with an acceptable model performance. We expect that this neither positively nor negatively influences our results concerning parameter transferability.

We define parameter transferability θ_{\leftrightarrow} as the percentage agreement in selected behavioural sets:

$$\theta_{\leftrightarrow} = \#(A_{S_i, T_j} \cap B_{S_k, T_l}) / n \cdot 100, \quad (6)$$

in which A_{S_i, T_j} is the set of selected behavioural members for spatial resolution S_i and temporal resolution T_j , and B_{S_k, T_l} are the selected members for spatial resolution S_k and temporal resolution T_l . The n is the total number of selected members (in this case, 32). Equation (6) expresses θ_{\leftrightarrow} as a percentage; if $\theta_{\leftrightarrow} = 100$, this indicates that for two different resolutions (either spatial, temporal or both), exactly the same parameter sets were selected as behavioural.

5 Results

First, the impact of temporal and spatial resolution on model performance is discussed for both uniform and distributed forcing, followed by a discussion of the impact of the temporal and spatial resolution on parameter distribution. For these analyses, the temporal and spatial resolution are assumed to be independent. Subsequently, the parameter transferability across temporal and spatial resolution is assessed by determining the overlap in behavioural sets as defined by Eq. (6). After that, parameter transferability over both temporal and spatial resolution is assessed. Finally, we investigate parameter transferability over the sub-basins of the Thur.

5.1 Impact of temporal and spatial resolution on model performance and parameter distribution

Figure 6 shows the model performance of the behavioural sets for the different spatial and temporal resolutions and the different objective functions, both for uniform and distributed forcing. We will first discuss the results for the uniform forcing.

With uniform forcing, the lumped model outperforms the distributed models for all three objective functions and time steps. The monthly time step shows for all three objective functions an increasing model performance with decreasing spatial resolution. It is remarkable that the model with the monthly time step outperforms the models with daily and hourly time steps when the $NSE(\log Q)$ was used as an objective function, while with the $NSE(Q)$ as an objective function exactly the opposite is the case. It is important to notice here that the monthly model results are simply an aggregation from the hourly model results, which might imply that the higher score on the monthly time step is the result of errors which compensate for each other, and that the model performance scores for the monthly time step are based on a considerable lower number of points. The $KGE(Q)$ as an objective function does not lead to a significantly different model performance for the monthly time step. From the figure it seems that both the spatial and temporal resolution have impact on the model performance. This is confirmed with a statistical test. An ANOVA analysis with two factors (temporal resolution, spatial resolution), with three or four levels (hourly, daily, monthly; $1 \text{ km} \times 1 \text{ km}$, $5 \text{ km} \times 5 \text{ km}$, $10 \text{ km} \times 10 \text{ km}$ and lumped) shows that both the spatial and temporal resolution have a significant ($p < 0.05$) impact on all three objective functions.

Distributed forcing leads in all cases except one ($1 \text{ km} \times 1 \text{ km}$, monthly, $NSE(\log Q)$) to an improved model performance compared to uniform forcing. It is important to note that for the lumped model uniform and distributed forcing are the same. It should therefore be remarked that while with uniform forcing the lumped model outperforms

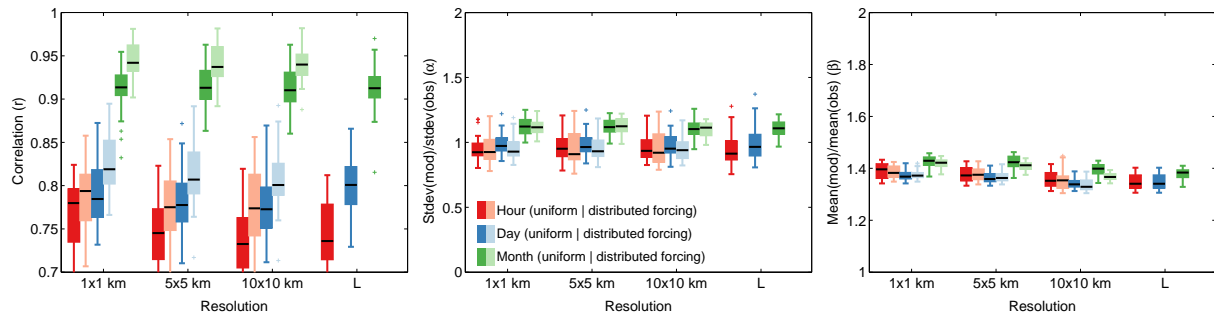


Figure 7. The model performance for the three separate components of the Kling–Gupta efficiency of the behavioural sets for different temporal and spatial resolutions. The left panel shows the correlation r , the middle panel the standard deviation of the model output divided by the standard deviation of the observations (α), and the right panel shows the mean of the model output divided by the mean of the observations (β).

the other model set-ups, for the distributed forcing the 10 km \times 10 km model outperforms the other spatial resolutions (except for $\text{NSE}(\log Q)$). An ANOVA analysis confirmed that also for distributed forcing, both spatial and temporal resolution have a significant ($p < 0.05$) impact on the model performance for all three objective functions.

Figure 7 shows the distribution of the behavioural sets for the three separate components of the $\text{KGE}(Q)$. Regarding the correlation r , the monthly time step scores higher than the daily and hourly time step. On the other hand, the hourly and daily time steps score higher with respect to β (closer towards 1). Although Fig. 6 gives the impression that the model performance in terms of $\text{KGE}(Q)$ is relatively insensitive to temporal and spatial resolution, Fig. 7 reveals this is actually the result of compensations from the three different components of the $\text{KGE}(Q)$: the monthly time step has a higher correlation, while the daily and hourly time steps have a higher β .

Figure 8 shows the parameter distribution of the seven sampled parameters, and shows how the distribution varies as a function of temporal and spatial resolution, both for distributed and uniform forcing. The distribution of the behavioural parameter sets for the daily and hourly time steps are very much alike for all parameters, but the distribution for the monthly time step is in some cases broader, which implies that the parameters are less clearly defined. The parameter showing the clearest effect of temporal scale is the advection coefficient C (Fig. 8). The C parameter, the velocity component in the routing, becomes less well defined with an increasing time step, which is intuitive because timing becomes less relevant for longer time intervals.

The difference in the parameter distribution when comparing distributed and uniform forcing is limited. The clearest difference can be found for the d_m parameter with the $\text{NSE}(Q)$ as an objective function. This parameter describes the maximum velocity of the baseflow, and can potentially impact short-term processes for which distributed forcing seems important, like surface runoff. However, there are

other parameters, such as the b_i parameter, which are more directly linked to infiltration and surface runoff processes and do not show a clear difference in parameter distribution between distributed and uniform forcing.

With an ANOVA analysis, the significance of temporal and spatial resolutions in the parameter distribution of the behavioural sets was tested. Figure 9 shows that the significance of spatial and temporal resolutions in the parameter distribution depends on which objective function was used to determine the behavioural sets. Uniform and distributed forcings show comparable patterns. In general, the temporal resolution has more impact on the parameter distribution (at least four parameters are significantly affected by temporal resolution) than the spatial resolution (only one parameter for one objective function experiences significant impact of the spatial resolution). Only two parameters are significantly impacted by the temporal resolution for all three objective functions: d_s and C .

5.2 Parameter transferability

The main research question of this study is to what extent parameters are transferable across temporal and spatial resolutions, and we will use that as an indicator of the representation of spatial and temporal variability in the model. We have defined parameter transferability θ_{\leftrightarrow} as the percentage agreement in identified behavioural sets (Eq. 6). Tables 2 and 3 give an overview of θ_{\leftrightarrow} for different temporal and spatial resolutions, both for uniform and distributed forcing. Table 2 shows that the θ_{\leftrightarrow} is generally high for different spatial resolutions, which suggests that the parameters are to a large extent transferable across spatial scales. In contrast, Table 3 shows that parameters are hardly transferable over the temporal scale. The selected runs for hourly and daily time steps largely agree, but the selected runs on a monthly time step are clearly different. Surprisingly, this is also strongly related to the objective function. The selection based on the $\text{NSE}(\log Q)$ is less sensitive to temporal resolution than those based on the $\text{KGE}(Q)$ or the $\text{NSE}(Q)$. A possible explanation

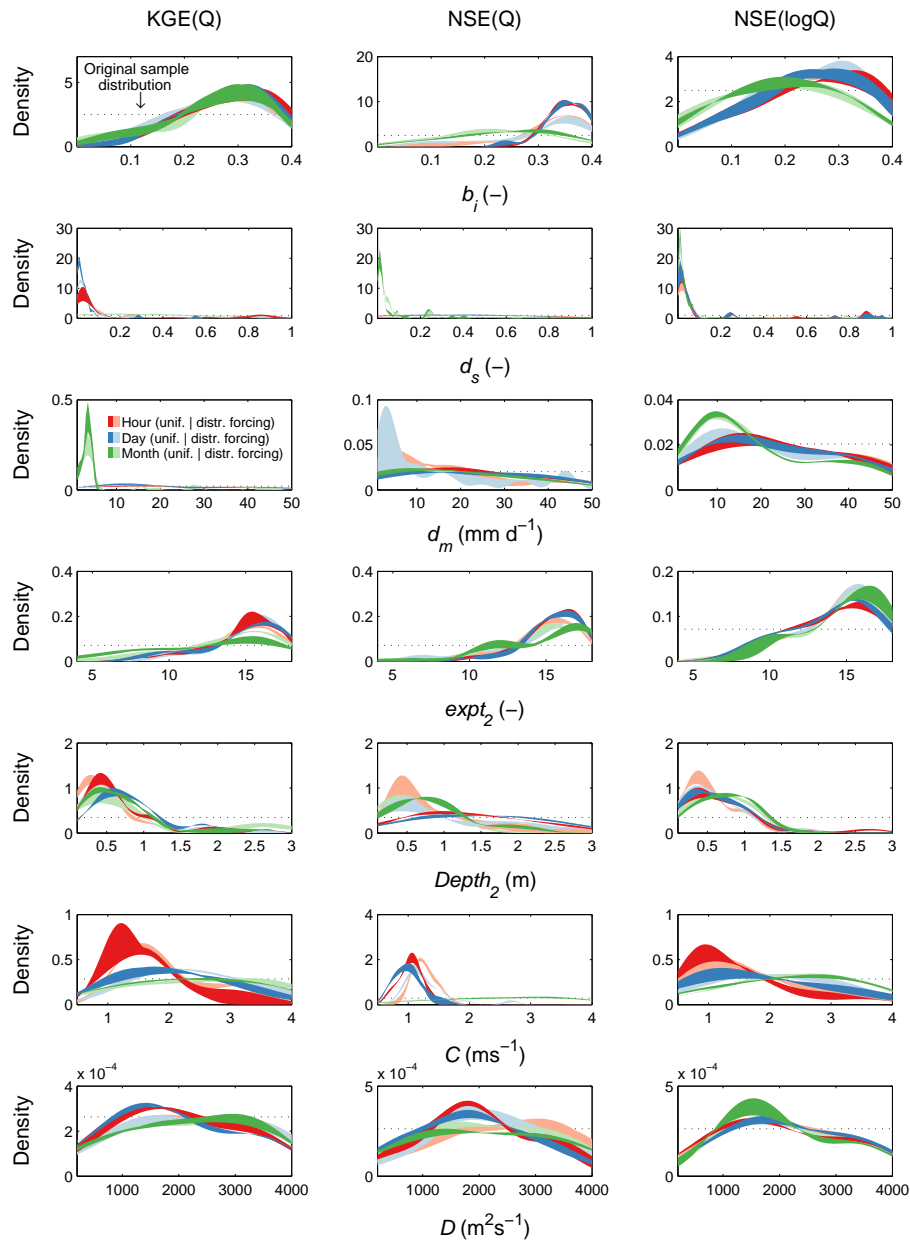


Figure 8. Distribution of the sampled parameters for the behavioural sets, fitted with a kernel density. The width of the line indicates the variation in distribution between the different spatial resolutions. The left column is based on $KGE(Q)$, the middle column on $NSE(Q)$ and the right column on $NSE(\log Q)$.

is that the $NSE(\log Q)$ tends to put more focus on lower discharges with a longer timescale, with less focus on the short-term flashy response of a catchment. Parameter transferability over space is in general slightly lower when distributed forcing is used compared to uniform forcing. On the other hand, parameter transferability over time is slightly higher for distributed forcing. Decreased sensitivity for the temporal resolution and increased sensitivity for the spatial resolution can indicate an improved physical representation with dis-

tributed forcing compared to uniform forcing, as one would expect.

Tables 2 and 3 list the parameter transferability over only one dimension (either spatial resolution or temporal resolution). We also investigated the combined effect of transferring parameters over both the spatial and temporal resolution. Figure 10 shows the relative impact of temporal and spatial resolution on parameter transferability based on $KGE(Q)$ for uniform forcing. To illustrate the relative impact of changes in spatial and temporal resolution, we fitted a linear surface

Table 2. Transferability of parameters across spatial resolution, expressed as percentage agreement in detected behavioural runs for different spatial resolutions (in km) at different time steps.

	Uniform forcing (% agreement)			Distributed forcing (% agreement)		
	KGE(Q)	NSE(Q)	NSE(log Q)	KGE(Q)	NSE(Q)	NSE(log Q)
Hour						
1 × 1 vs. 5 × 5	78	84	91	88	75	84
1 × 1 vs. 10 × 10	72	81	81	78	56	78
5 × 5 vs. 10 × 10	94	94	91	88	81	94
1 × 1 vs. lumped	78	88	91			
5 × 5 vs. lumped	91	84	94			
10 × 10 vs. lumped	88	81	88			
Day						
1 × 1 vs. 5 × 5	94	84	84	91	84	91
1 × 1 vs. 10 × 10	84	69	69	78	69	81
5 × 5 vs. 10 × 10	91	84	84	89	84	91
1 × 1 vs. lumped	1	81	88			
5 × 5 vs. lumped	91	88	94			
10 × 10 vs. lumped	84	84	81			
Month						
1 × 1 vs. 5 × 5	75	88	88	84	84	91
1 × 1 vs. 10 × 10	66	84	81	66	78	84
5 × 5 vs. 10 × 10	88	91	94	78	88	94
1 × 1 vs. lumped	78	72	94			
5 × 5 vs. lumped	78	75	88			
10 × 10 vs. lumped	78	78	88			

Table 3. Transferability of parameters across temporal resolution, expressed as percentage agreement in detected behavioural runs for different temporal resolutions at different spatial resolutions.

	Uniform forcing (% agreement)			Distributed forcing (% agreement)		
	KGE(Q)	NSE(Q)	NSE(log Q)	KGE(Q)	NSE(Q)	NSE(log Q)
1 km × 1 km						
Hour vs. day	56	81	81	69	63	75
Hour vs. month	3	6	34	6	9	47
Day vs. month	3	6	47	6	13	63
5 km × 5 km						
Hour vs. day	66	88	81	69	69	81
Hour vs. month	3	6	38	9	6	53
Day vs. month	3	6	47	9	6	66
10 km × 10 km						
Hour vs. day	63	75	78	59	72	78
Hour vs. month	3	3	44	13	6	59
Day vs. month	0	6	63	13	6	75
Lumped						
Hour vs. day	66	84	81			
Hour vs. month	3	0	44			
Day vs. month	3	3	53			

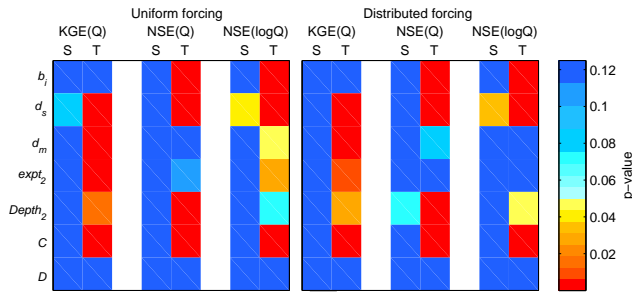


Figure 9. The effect of spatial and temporal resolutions on parameter distribution. The p value indicates the significance of the impact of spatial resolution (S) and temporal resolution (T) on the parameter values of the behavioural sets, evaluated for the three objective functions.

through the data points from our study ($R^2 = 0.68$). The figure clearly shows that temporal resolution has a stronger impact on parameter transferability than spatial resolution. The linear regression equation that describes the surface in Fig. 10 is given below:

$$\theta_{\leftrightarrow KGE(Q)} = 83.3 - 12.6 \cdot \frac{T_j}{T_l} - 3.0 \cdot \frac{S_i}{S_k}, \quad (7)$$

in which $\frac{T_j}{T_l}$ is the ratio in temporal resolution between the two model set-ups over which parameters are transferred and $\frac{S_i}{S_k}$ is the ratio in spatial resolution (L/L) between the two model set-ups. The effect of temporal resolution on parameter transferability is stronger (slope of 12.6) than the effect of spatial resolution (slope of 3.0). Parameter transferability decreases when the ratio between the original and the intended spatial and temporal resolutions increases. The surfaces based on $NSE(Q)$ ($R^2 = 0.60$) and $NSE(\log Q)$ ($R^2 = 0.75$) show a similar behaviour:

$$\theta_{\leftrightarrow NSE(Q)} = 88.6 - 12.8 \cdot \frac{T_j}{T_l} - 2.8 \cdot \frac{S_i}{S_k}, \quad (8)$$

$$\theta_{\leftrightarrow NSE(\log Q)} = 92.9 - 7.4 \cdot \frac{T_j}{T_l} - 3.6 \cdot \frac{S_i}{S_k}. \quad (9)$$

When we fit a surface through the points obtained for the models run with distributed forcing, the linear regression equations ($R^2 = 0.66, 0.67, 0.88$ respectively) look as follows:

$$\theta_{\leftrightarrow KGE(Q)} = 80.3 - 11.4 \cdot \frac{T_j}{T_l} - 2.6 \cdot \frac{S_i}{S_k}, \quad (10)$$

$$\theta_{\leftrightarrow NSE(Q)} = 75.3 - 10.3 \cdot \frac{T_j}{T_l} - 4.3 \cdot \frac{S_i}{S_k}, \quad (11)$$

$$\theta_{\leftrightarrow NSE(\log Q)} = 91.3 - 5.4 \cdot \frac{T_j}{T_l} - 2.8 \cdot \frac{S_i}{S_k}. \quad (12)$$

Also for the models with distributed forcing, the slope for the temporal resolution is steeper than the slope for spatial resolution, implying that parameter transferability is more sensitive for temporal resolution than for spatial resolution. Compared to uniform forcing, the slope for temporal resolution,

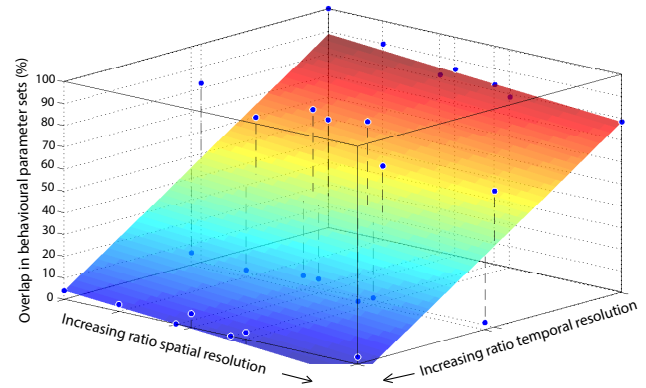


Figure 10. Parameter transferability as a function of the ratio in temporal and spatial resolution. The ratio of temporal resolutions is defined as follows: transfer from hourly to daily time steps is a ratio of 24, whereas transfer from hourly to monthly is a ratio of 732 (732 h in 1 month of 30.5 days). The ratio of spatial resolutions is defined as the square root of the number of cells that would fit in the other cell: from $1 \text{ km} \times 1 \text{ km}$ resolution to $5 \text{ km} \times 5 \text{ km}$ resolution is a ratio of $\sqrt{25} = 5$. The behavioural sets were determined based on the $KGE(Q)$. The linear surface ($R^2 = 0.68$) was fitted to illustrate the relative impact of changes in spatial and temporal resolution.

and hence the impact of temporal resolution on transferability, is less steep for distributed forcing, while the slope for spatial resolution is on average comparable for both forcings.

5.3 Spatially distributed parameters

The advantage of distributed hydrological models over lumped models is that distributed models can incorporate spatially varying parameters, including those reflecting land-use and soil characteristics (Carpenter and Georgakakos, 2006), and spatially varying forcing. Figure 11 for example shows how the spatial variation in bulk density decreases with increasing resolution. However, in this study, as in most large-domain studies with distributed models, the most sensitive parameters (i.e. the ones that were calibrated) have been applied uniformly over the grid cells. The main motivation for this practice is the ill-posedness of the problem (too many parameters have to be identified with too little information), in addition to computational time. This implies that the advantage of a distributed model remains unused for the parameters that impact the model output most. To test the spatial distribution of the most sensitive parameters for the Thur basin, we have investigated parameter transferability between the Thur basin and the nine subbasins for which discharge data were available (see Sect. 2.1 and Fig. 2). Table 4 gives an overview of a selected number of spatial and temporal resolutions. The table shows that parameter transferability from the Thur to the subbasins is notably low. An extreme example is the St. Gallen catchment, which has a maximum of one behavioural parameter set in common with the Thur basin. Table 4 therefore shows that the spatial vari-

Table 4. Transferability of parameters from the Thur to the nine subbasins, expressed as percentage agreement (%) in detected behavioural runs. The forcing was applied uniformly and the $KGE(Q)$ was used as an objective function.

Catchment (size)	1 km × 1 km			5 km × 5 km	10 km × 10 km
	Hour	Day	Month	Hour	Hour
Rietholzbach (3.3 km ²)	19	0	0	25	19
Herisau (17.8 km ²)	16	6	0	16	16
Appenzell (74.2 km ²)	28	25	9	28	16
Wängi (78.9 km ²)	9	56	31	34	50
Mogelsberg (88.2 km ²)	28	38	66	19	28
Frauenfeld (212 km ²)	3	3	75	3	0
St. Gallen (261 km ²)	3	0	0	3	0
Jonschwil (493 km ²)	6	0	0	6	0
Halden (1085 km ²)	19	9	0	18	13

ation in the calibrated parameters is underestimated in the current model set-up.

6 Discussion

6.1 Model performance

It seems counter-intuitive that model performance is significantly affected by both the temporal and spatial resolution, while the parameter distribution is mainly impacted by the temporal resolution. This can be explained, however. Model performance can still be significantly impacted by temporal and spatial resolution, even if the same parameters are selected for different spatial resolutions. This implies that the model performance is mainly limited by the model structure or set-up, and much less by the parameter values. This is confirmed by comparing the uniform and distributed forcing. Although the distribution of the behavioural parameters was not very different for the two forcing types, the model performance for distributed forcing was in almost all cases better than the model performance for the uniform forcing.

Liang et al. (2004) defined a so-called “critical resolution”, beyond which a finer spatial resolution would not lead to any improvement in the model performance. In the study of Liang et al. (2004) this critical resolution for the VIC model was found to be $1/8^\circ$ ($\approx 12.5 \text{ km} \times 12.5 \text{ km}$). All spatial resolutions applied in this study, but the lumped ones are below this critical resolution. The results in this study are therefore consistent with the results from Liang et al. (2004), because we did not find any improvement in model performance with increasing spatial resolution, neither for the uniform nor for the distributed forcing. Rather, we find the contrary; for the uniform forcing the lumped model outperformed the higher-resolution models, and for the distributed forcing the $10 \text{ km} \times 10 \text{ km}$ outperformed the other models. If something like a critical resolution exists, it is probably related to the processes represented in the model. Con-

trary to our findings are the results of Zappa (2002), who found that a critical spatial resolution in the Thur region is of the order of $500 \text{ m} \times 500 \text{ m}$ using the PREVAH model, because of the complex topography and snow processes in the catchment. This can either imply that the sub-grid variability parametrization in VIC is effective, or that not all relevant hydrological processes are included in the VIC model. In order to check this last suggestion, future research on parameter transferability should consider more hydrological fluxes and states besides the discharge, e.g. evapotranspiration.

6.2 The high sensitivity for temporal resolution

The conclusion that parameters cannot be transferred across temporal resolution seems to contradict the results of Troy et al. (2008). The large difference is that Troy et al. (2008) only used sub-daily time steps (1, 3, 6, 12 h), whereas we did find agreement between the hourly and daily time steps. Therefore, our results are not necessarily contradictory. Troy et al. (2008) chose the sub-daily time steps in order to investigate whether time could be saved in the calibration process by calibrating on a coarser time step. Unfortunately, the reality is that in most large-domain studies models are calibrated with monthly discharge observations (Melsen et al., 2016) rather than with sub-daily observations. Our results suggest that models which were calibrated or validated at a monthly time step cannot be interpreted at the daily or hourly time step. Chaney et al. (2015) showed that monthly discharge observations could decrease the uncertainty around the daily flow duration curve. The decrease in uncertainty by adding monthly discharge information differed for different climates. The Thur basin, with a wet continental climate, would experience a high reduction in uncertainty. This means that our results, which show that with monthly data it is impossible to determine the optimal parameter set for the hourly or daily time step, would even be stronger for dry climates (Chaney et al., 2015). Kavetski et al. (2011) showed that parameter values can significantly change by changing

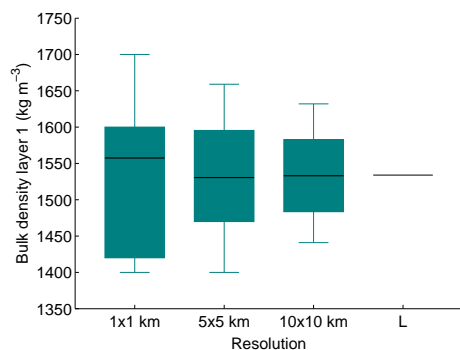


Figure 11. Distribution of bulk density over the grid cells for the four different spatial resolutions.

the temporal resolution. They found that the sensitivity of a parameter to temporal resolution could be related to the model structure; the parameters from simpler model structures were more sensitive to temporal resolution than the parameters from more complex models.

Figure 12 and Tables S2 and S3 show that the conclusions we draw from Tables 2 and 3 are not only valid for the best 1 % of runs selected as behavioural. Tables S2 and S3 show that the same patterns are found when selecting the best 2 % or 5 % of the model runs. Figure 12 gives an overview for two selected cases, which show that model performance deteriorates when parameters are transferred over time, also for the best 10 % up to higher thresholds, whereas the impact of spatial resolution on model performance deterioration is limited.

6.3 Models vs. nature: do the current generation of models adequately represent spatial variability?

Our results show that parameter transferability is more sensitive to temporal than to spatial resolution. A key question is to what extent this result stems from the model representation of spatial variability. Spatial variability can be reflected in three domains of the model: the routing, the forcing, and the soil and land-use parameters. In this study we excluded the effect of routing by using a high-resolution drainage network based on sub-basins with a size of $\sim 1 \text{ km}^2$, independent of the resolution of the hydrologic model. We think that the effect of spatial resolution can be increased by adapting the routing scheme accordingly. Drainage network resolution may affect the projected hydrograph, for example with changes in the stream network and the channel slope. However, this effect should then be assigned to the routing model, and not to the runoff generation model (the hydrologic model). For clarity, we decided to exclude the effect of spatial resolution on routing in this study.

We investigated the effect of forcing by comparing the results for distributed and uniformly applied forcing, and we tested the effect of spatially distributed soil and land-use pa-

rameters by aggregating them for lower resolutions (Fig. 11). Despite distributed forcing and the decrease in variation in soil and land-use parameters, the model parameters showed low sensitivity to the spatial resolution. A possible explanation could be the sub-grid parametrizations of the VIC model for land use and elevation, which decrease the effect of up-scaling these parameters to other resolutions, as shown by Haddeland et al. (2002). However, we think that Sect. 5.3 and Table 4 show how spatial variability is underestimated by calibrating and applying the most sensitive parameters uniformly over the basin.

The models in this study are configured in a similar way to many current-day large-domain hydrological models, using common data like the Harmonized World Soil Database and uniform application of the most sensitive parameters. As such, this study is likely representative of many large-domain studies. The limited sensitivity for spatial resolution is arguable because our implementation of VIC substantially underestimates the spatial variability in nature, and, importantly, that similar issues in representing spatial variability are a common problem in large-domain hydrological modelling (e.g. see the model configuration in Mizukami et al., 2016). Many studies have considered spatial variability in forcing (Adams et al., 2012; Lobligeois et al., 2014) and soil parameters (Mohanty and Skaggs, 2001; Western et al., 2004). Kim et al. (1997) accounted for heterogeneity in soil hydraulic properties using stochastic methods, based on the scaling theory of Miller and Miller (1956). In fact, the effect of stochastic soil parametrizations on parameter transferability would be a valuable research topic (Maxwell and Kollet, 2008). We argue here that the high spatial transferability may occur because the current generation of land-surface models have an inadequate representation of spatial variability and hydrologic connectivity, providing a strong motivation to substantially improve the representation of spatial and temporal variability in models. This not only implies increasing the spatial (and temporal) resolution of the model, but also including more relevant hydrological processes. Promising techniques have been developed to allow spatial distribution of calibrated parameters, for example with multiscale parameter regionalization (MPR, Samaniego et al., 2010; Kumar et al., 2013), which could and should be applied for large-domain hydrologic models.

6.4 Limitations of this case study

The results in our study are based on a limited number of model configurations for a single basin, so the results presented here are only intended to provide an example of the behaviour in the current generation of land-surface models. Our results show a low sensitivity for the spatial resolution, whether applied with distributed forcing or not. The observed impact of spatial resolution can therefore almost completely be attributed to the effect of spatially distributed soil and land-use parameters (including the calibrated ones), which

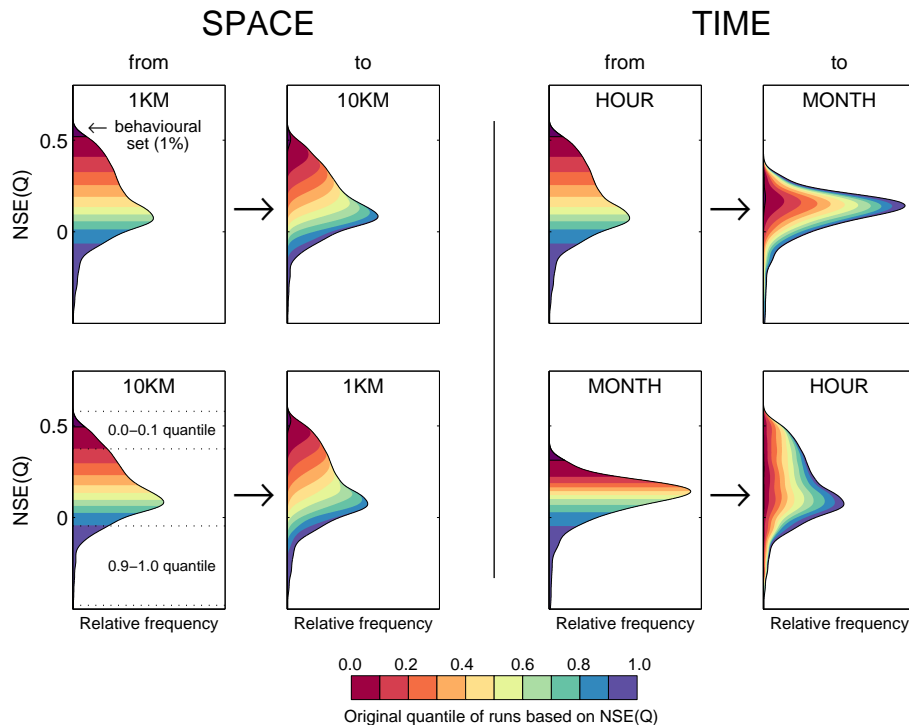


Figure 12. Impact of parameter transfer on model performance. The panels show the distribution of the $NSE(Q)$ fitted with a kernel density for 3150 runs. On the left-hand side of the arrow the red area represents the best 10 % of the runs, each colour interval increasing with 10 % to the full data set (100 %, purple). The selected behavioural runs are indicated separately with a black line (best 1 %). The panel on the right-hand side of the arrow shows the distribution of the model performance for the coloured selections when evaluated at another spatial (left panels) or temporal (right panels) resolution. When the direction of the colours changes from the left panel to the right panel, this implies a low parameter transferability. The data for the first two columns are based on hourly discharges; the data for the second two columns are based on the $1\text{ km} \times 1\text{ km}$ model.

could be substantially underestimated. The impact of temporal resolution on parameter transferability is large. We employed the temporal resolutions for which most hydrological observations are available; thus, our results are relevant for practical applications. Based on the work of Chaney et al. (2015) we expect that parameter transferability will be lower for arid climates than the numbers we obtained, and based on the work of Kavetski et al. (2011) we expect that parameter transferability will be lower for more parsimonious models. The general message from our study is the surprisingly high spatial transferability, highlighting the need for a focused research effort to improve the representation of spatial variability in large-domain distributed models (GHMs). A possible path forward is to develop computationally frugal process representations, as for example presented by Hazenberg et al. (2015) for hillslope processes.

7 Summary and conclusions

A VIC model for the Thur basin was run with four different spatial resolutions ($1\text{ km} \times 1\text{ km}$, $5\text{ km} \times 5\text{ km}$, $10\text{ km} \times 10\text{ km}$, lumped) and evaluated at three different tem-

poral resolutions (hourly, daily, monthly). The forcing was applied both uniformly and distributed over the catchment, and the drainage network for the routing model was defined independently of the hydrological model resolution. Three objective functions were used to evaluate model performance: $KGE(Q)$, $NSE(Q)$ and the $NSE(\log Q)$. The model was run 3150 times using the Hierarchical Latin Hypercube Sample and the best 1 % of the runs was selected as behavioural and used for further analysis. Parameter transferability was quantified by evaluating the overlap in behavioural sets for different temporal and spatial resolutions. From the results we can draw the following conclusions.

- Both the spatial resolution and the temporal resolution of the VIC model had a significant impact on the model performance, either expressed in terms of $KGE(Q)$, $NSE(Q)$, or $NSE(\log Q)$. The model performance evaluated at a monthly time step consistently increased with decreasing spatial resolution, while for the daily and hourly time step no clear relation to spatial resolution could be found. Generally, the models applied with spatially distributed forcing performed better than the models applied with uniform forcing.

- The spatial resolution of the model had little impact on the parameter distribution of the behavioural sets. On the other hand, the temporal resolution significantly impacted the distribution of at least four out of seven parameters, both when applied with uniform and distributed forcing.
- Parameters could to a large extent be transferred across the spatial resolutions, while parameter transferability over the temporal resolutions was less trivial. Parameter transferability between the hourly and daily time steps was found to be feasible, but the monthly time step led to substantially different parameter values. This is crucial information, because many studies tend to calibrate the VIC model on the monthly time step (Melsen et al., 2016). The results of this study suggest that the output from models calibrated on a monthly time step cannot be interpreted or analysed on a daily or hourly time step. This might seem obvious, but it should be recognized that the increasing spatial resolution of large-domain land-surface models might increase the expectations concerning temporal resolution as well, as described in Melsen et al. (2016).
- We also investigated whether parameters could be transferred across both the spatial and the temporal resolutions simultaneously. Parameter transferability decreases when the ratio between the original and the intended spatial and/or temporal resolution increases. The ratio of temporal resolutions has a larger negative effect on parameter transferability than the ratio of spatial resolutions. It was also shown that parameter transferability depends on the objective function. When the $NSE(\log Q)$, which tends to put more emphasis on low flows, is used as an evaluation criterion, the parameter values at a monthly time step overlap much more with the daily and hourly time steps than when $KGE(Q)$ or $NSE(Q)$ are used as objective functions. This means that parameter transferability across temporal resolution also depends on the timescale of the process to which a particular parameter refers.

The most important result of our study is that it showed high parameter transferability across spatial resolution, even when forcing was applied in a distributed fashion. A possible explanation for the low sensitivity to spatial resolution is the uniform application of the most sensitive parameters. This is indicative of a substantial underestimation of the actual spatial variability represented by the VIC simulations. We did, however, construct our model according to current-day standards for large-domain land-surface models, raising the point that the high spatial transferability may occur because the current generation of models has an inadequate representation of spatial variability and hydrologic connectivity. The results presented in this paper provide strong motivation to further investigate and substantially improve the representa-

tion of spatial and temporal variability in large-domain hydrological models. Large-domain hydrological models have many applications, from water footprints (Gleeson et al., 2012) and water scarcity (Hoekstra, 2014), to global water use (Wada and Bierkens, 2014) and electricity supply (Van Vliet et al., 2012), but the spatial variability in the models is very likely underestimated, which increases the uncertainty in the model results. A critical evaluation of large-domain hydrological models on a smaller scale, as conducted in this study, shows that we should be careful with interpreting the results of large-domain models.

The Supplement related to this article is available online at doi:10.5194/hess-20-2207-2016-supplement.

Acknowledgements. The authors would like to thank Kevin Sampson for the preparation of GIS files for the routing, Oldrich Rakovec for providing and helping with DELSA, and Miroslav Voráček for the provided Hierarchical Latin Hypercube Sample. The Swiss Federal Office for the Environment (FOEN) and Martin Hirschi and Dominic Michel from ETH Zürich are thanked for kindly providing the discharge data. We would like to thank MeteoSwiss for providing the forcing data. Lieke Melsen would like to acknowledge Niko Wanders, Wouter Greuell, Pablo Mendoza, Rohini Kumar, Stephan Tober and Oldrich Rakovec for fruitful discussions that led to the basis of this paper. The data in this study are available from the first author upon request.

Edited by: M. Weiler

References

- Abbaspour, K., Yang, J., Maximov, I., Siber, R., Bogner, K., Mieleitner, J., Zobrist, J., and Srinivasan, R.: Modelling hydrology and water quality in the pre-alpine/alpine Thur watershed using SWAT, *J. Hydrol.*, 333, 413–430, doi:10.1016/j.jhydrol.2006.09.014, 2007.
- Adams, R., Western, A., and Seed, A.: An analysis of the impact of spatial variability in rainfall on runoff and sediment predictions from a distributed model, *Hydrol. Process.*, 26, 3263–3280, doi:10.1002/hyp.8435, 2012.
- Andersen, O., Seneviratne, S., Hinderer, J., and Viterbo, P.: GRACE-derived terrestrial water storage depletion associated with the 2003 European heat wave, *Geophys. Res. Lett.*, 32, L18405, doi:10.1029/2005GL023574, 2005.
- Becker, A. and Grünwald, U.: Flood risk in Central Europe, *Science*, 300, 1099, doi:10.1126/science.1083624, 2003.
- Bennett, J., Robertson, D., Ward, P., Hapuarachchi, H., and Wang, Q.: Calibrating hourly rainfall-runoff models with daily forcings for streamflow forecasting applications in meso-scale catchments, *Environ. Model. Softw.*, 76, 20–36, doi:10.1016/j.envsoft.2015.11.006, 2016.

- Beven, K. J. and Binley, A.: The future of distributed models: Model calibration and uncertainty prediction, *Hydrol. Process.*, 6, 279–298, doi:10.1002/hyp.3360060305, 1992.
- Beven, K. J. and Binley, A.: GLUE: 20 years on, *Hydrol. Process.*, 28, 5897–5918, doi:10.1002/hyp.10082, 2014.
- Beven, K. J.: *Rainfall-Runoff modelling, The Primer*, 2nd Edn., chap. 1, *Down to Basics: Runoff Processes and the Modelling Process*, John Wiley & Sons, Chichester, West Sussex, UK, 1–22, 2012.
- Bierkens, M. F. P.: Global hydrology 2015: State, trends, and directions, *Water Resour. Res.*, 51, 4923–4947, doi:10.1002/2015WR017173, 2015.
- Bierkens, M. F. P., Bell, V., Burek, P., Chaney, N., Condon, L., David, C., De Roo, A., Döll, P., Drost, N., Famiglietti, J., Flörke, M., Gochis, D., Houser, P., Hut, R., Keune, J., Kollet, S., Maxwell, R., Reager, J., Samaniego, L., Sudicky, E., Sutanudjaja, E., Van de Giesen, N., Winsemius, H., and Wood, E.: Hyper-resolution global hydrological modelling: What's next?, *Hydrol. Process.*, 29, 310–320, doi:10.1002/hyp.10391, 2014.
- Boyle, D., Gupta, H., Sorooshian, S., Koren, V., Zhang, Z., and Smith, M.: Towards improved streamflow forecasts: Value of semidistributed modeling, *Water Resour. Res.*, 37, 2749–2759, doi:10.1029/2000WR000207, 2001.
- Carpenter, T. and Georgakakos, K.: Intercomparison of lumped versus distributed hydrologic model ensemble simulations on operational forecast scales, *J. Hydrol.*, 329, 174–185, doi:10.1016/j.jhydrol.2006.02.013, 2006.
- Chaney, N. W., Herman, J. D., Reed, P. M., and Wood, E. F.: Flood and drought hydrologic monitoring: the role of model parameter uncertainty, *Hydrol. Earth Syst. Sci.*, 19, 3239–3251, doi:10.5194/hess-19-3239-2015, 2015.
- Costa-Cabral, M., Roy, S., Maurer, E., Mills, W., and Chen, L.: Snowpack and runoff response to climate change in Owens Valley and Mono Lake watersheds, *Climatic Change*, 116, 97–109, doi:10.1007/s10584-012-0529-y, 2013.
- Demaria, E. M., Nijssen, B., and Wagener, T.: Monte Carlo sensitivity analysis of land surface parameters using the Variable Infiltration Capacity model, *J. Geophys. Res.*, 112, D11113, doi:10.1029/2006JD007534, 2007.
- Duan, Q., Schaake, J., Andréassian, V., Franks, S., Goteti, G., Gupta, H., Gusev, Y., Habets, F., Hall, A., Hay, L., Hogue, T., Huang, M., Leavesley, G., Liang, X., Nasonova, O., Noilhan, J., Oudin, L., Sorooshian, S., Wagener, T., and Wood, E.: Model Parameter Estimation Experiment (MOPEX): An overview of science strategy and major results from the second and third workshops, *J. Hydrol.*, 320, 3–17, doi:10.1016/j.jhydrol.2005.07.031, 2006.
- FAO, IIASA, ISRIC, ISSCAS, and JRC: *Harmonized World Soil Database (version 1.2)*, Tech. rep., AO, Rome, Italy and IIASA, Laxenburg, Austria, <http://www.fao.org/soils-portal/soil-survey/soil-maps-and-databases/harmonized-world-soil-database-v12/en/> (last access: 14 March 2014), 2012.
- Ficchi, A., Perrin, C., and Andréassian, V.: Impact of temporal resolution of inputs on hydrological model performance: An analysis based on 2400 flood events, *J. Hydrol.*, 538, 454–470, doi:10.1016/j.jhydrol.2016.04.016, 2016.
- Finnerty, B., Smith, M., Sea, D., Koren, V., and Moglen, G.: Space-time scale sensitivity of the Sacramento model to radar-gage precipitation inputs, *J. Hydrol.*, 203, 21–38, doi:10.1016/S0022-1694(97)00083-8, 1997.
- Francini, M. and Pacciani, M.: Comparative analysis of several conceptual rainfall-runoff models, *J. Hydrol.*, 122, 161–219, 1991.
- Fundel, F. and Zappa, M.: Hydrological ensemble forecasting in mesoscale catchments: Sensitivity to initial conditions and value of reforecasts, *Water Resour. Res.*, 47, W09520, doi:10.1029/2010WR009996, 2011.
- Fundel, F., Jörg-Hess, S., and Zappa, M.: Monthly hydrometeorological ensemble prediction of streamflow droughts and corresponding drought indices, *Hydrol. Earth Syst. Sci.*, 17, 395–407, doi:10.5194/hess-17-395-2013, 2013.
- Gleeson, T., Wada, Y., and van Beek, M. P. B. L. H.: Water balance of global aquifers revealed by groundwater footprint, *Nature*, 488, 197–200, doi:10.1038/nature11295, 2012.
- Gupta, H., Kling, H., Yilmaz, K., and Martinez, G.: Decomposition of the mean squared error and NSE performance criteria: Implications for improving hydrological modelling, *J. Hydrol.*, 377, 80–91, 2009.
- Gurtz, J., Baltensweiler, A., and Lang, H.: Spatially distributed hydrotope-based modelling of evapotranspiration and runoff in mountainous basins, *Hydrol. Process.*, 13, 2751–2768, 1999.
- Gurtz, J., Verbunt, M., Zappa, M., Moesch, M., Pos, F., and Moser, U.: Long-term hydrometeorological measurements and model-based analyses in the hydrological research catchment Rietholzbach, *J. Hydrol. Hydromech.*, 51, 162–174, 2003.
- Haddeland, I., Matheussen, B., and Lettenmaier, D.: Influence of spatial resolution on simulated streamflow in a macroscale hydrologic model, *Water Resour. Res.*, 38, 1124, doi:10.1029/2001WR000854, 2002.
- Haddeland, I., Lettenmaier, D., and Skaugen, T.: Reconciling Simulated Moisture Fluxes Resulting from Alternate Hydrologic Model Time Steps and Energy Budget Closure Assumptions, *J. Hydrometeorol.*, 7, 355–370, doi:10.1175/JHM496.1, 2006.
- Hazenbergh, P., Fang, Y., Broxton, P., Gochis, D., Niu, G., Pelletier, J., Troch, P., and Zeng, X.: A hybrid-3D hillslope hydrological model for use in Earth system models, *Water Resour. Res.*, 10, 8218–8239, doi:10.1002/2014WR016842, 2015.
- Hoekstra, A.: Water scarcity challenges to business, *Nat. Clim. Change*, 4, 318–320, doi:10.1038/nclimate2214, 2014.
- Hurkmans, R. T. W. L., de Moel, H., Aerts, J. C. J. H., and Troch, P. A.: Water balance versus land surface model in the simulation of Rhine river discharges, *Water Resour. Res.*, 44, W01418, doi:10.1029/2007WR006168, 2008.
- Jasper, K., Calanca, P., Gyalistras, D., and Fuhrer, J.: Differential impacts of climate change on the hydrology of two Alpine river basins, *Clim. Res.*, 26, 113–129, doi:10.3354/cr026113, 2004.
- Jörg-Hess, S., Kempf, S., Fundel, F., and Zappa, M.: The benefit of climatological and calibrated reforecast data for simulating hydrological droughts in Switzerland, *Meteorol. Appl.*, 22, 444–458, doi:10.1002/met.1474, 2015.
- Kavetski, D., Fenicia, F., and Clark, M. P.: Impact of temporal data resolution on parameter inference and model identification in conceptual hydrological modeling: Insights from an experimental catchment, *Water Resour. Res.*, 47, W05501, doi:10.1029/2010WR009525, 2011.
- Kim, C. P., Stricker, J. N. M., and Feddes, R. A.: Impact of soil heterogeneity on the water budget of the unsaturated zone, *Water Resour. Res.*, 33, 991–999, doi:10.1029/97WR00364, 1997.

- Krause, P., Boyle, D. P., and Båse, F.: Comparison of different efficiency criteria for hydrological model assessment, *Adv. Geosci.*, 5, 89–97, doi:10.5194/adgeo-5-89-2005, 2005.
- Kumar, R., Samaniego, L., and Attinger, S.: Implications of distributed hydrologic model parameterization on water fluxes at multiple scales and locations, *Water Resour. Res.*, 49, 360–379, doi:10.1029/2012WR012195, 2013.
- Liang, X., Lettenmaier, D. P., Wood, E. F., and Burges, S. J.: A simple hydrologically based model of land surface water and energy fluxes for general circulation models, *J. Geophys. Res.*, 99, 14415–14458, 1994.
- Liang, X., Wood, E. F., and Lettenmaier, D. P.: Surface soil moisture parameterization of the VIC-2L model: Evaluation and modification, *Global Planet. Change*, 13, 195–206, doi:10.1016/0921-8181(95)00046-1, 1996.
- Liang, X., Guo, J., and Leung, L.: Assessment of the effects of spatial resolutions on daily water flux simulations, *J. Hydrol.*, 298, 287–310, doi:10.1016/j.jhydrol.2003.07.007, 2004.
- Littlewood, I. and Croke, B.: Data time-step dependency of conceptual rainfall-streamflow model parameters: an empirical study with implications for regionalisation, *Hydrolog. Sci. J.*, 53, 685–695, doi:10.1623/hysj.53.4.685, 2008.
- Littlewood, I. and Croke, B.: Effects of data time-step on the accuracy of calibrated rainfall-streamflow model parameters: practical aspects of uncertainty reduction, *Hydrol. Res.*, 44, 430–440, doi:10.2166/nh.2012.099, 2013.
- Liu, H., Tian, F., Hu, H., Hu, H., and Sivapalan, M.: Soil moisture controls on patterns of grass green-up in Inner Mongolia: an index based approach, *Hydrol. Earth Syst. Sci.*, 17, 805–815, doi:10.5194/hess-17-805-2013, 2013.
- Liu, Y. and Gupta, H. V.: Uncertainty in hydrologic modeling: Towards an integrated data assimilation framework, *Water Resour. Res.*, 43, W07401, doi:10.1029/2006WR005756, 2007.
- Lobligeois, F., Andréassian, V., Perrin, C., Tabary, P., and Loumagne, C.: When does higher spatial resolution rainfall information improve streamflow simulation? An evaluation using 3620 flood events, *Hydrol. Earth Syst. Sci.*, 18, 575–594, doi:10.5194/hess-18-575-2014, 2014.
- Lohmann, D., Nolte-Holube, R., and Raschke, E.: A large-scale horizontal routing model to be coupled to land surface parameterization schemes, *Tellus A*, 48, 708–721, 1996.
- Maxwell, R. and Kollet, S.: Quantifying the effects of three-dimensional subsurface heterogeneity on Hortonian runoff processes using a coupled numerical, stochastic approach, *Adv. Water Resour.*, 31, 807–817, doi:10.1016/j.advwatres.2008.01.020, 2008.
- Melsen, L., Teuling, A., van Berkum, S., Torfs, P., and Uijlenhoet, R.: Catchments as simple dynamical systems: A case study on methods and data requirements for parameter identification, *Water Resour. Res.*, 50, 5577–5596, doi:10.1002/2013WR014720, 2014.
- Melsen, L., Teuling, A., Torfs, P., Uijlenhoet, R., Mizukami, N., and Clark, M.: HESS Opinions: The need for process-based evaluation of large-domain hyper-resolution models, *Hydrol. Earth Syst. Sci.*, 20, 1069–1079, doi:10.5194/hess-20-1069-2016, 2016.
- Miller, E. and Miller, R.: Physical theory for capillary flow phenomena, *J. Appl. Phys.*, 27, 324–332, doi:10.1063/1.1722370, 1956.
- Miralles, D., Teuling, A., van Heerwaarden, C., and Vilà-Guerau de Arellano, J.: Mega-heatwave temperatures due to combined soil desiccation and atmospheric heat accumulation, *Nat. Geo. Sci.*, 7, 345–349, doi:10.1038/ngeo2141, 2014.
- Mizukami, N., Clark, M. P., Sampson, K., Nijssen, B., Mao, Y., McMillan, H., Viger, R. J., Markstrom, S. L., Hay, L. E., Woods, R., Arnold, J. R., and Brekke, L. D.: mizuRoute version 1: a river network routing tool for a continental domain water resources applications, *Geosci. Model Dev. Discuss*, 8, 9415–9449, doi:10.5194/gmdd-8-9415-2015, 2015.
- Mizukami, N., Clark, M., Gutmann, E., Mendoza, P., Newman, A., Nijssen, B., Livneh, B., Hay, L., Arnold, J., and Brekke, L.: Implications of the methodological choices for hydrologic portrayals of climate change over the contiguous United States: Statistically downscaled forcing data and hydrologic models, *J. Hydrometeorol.*, 17, 73–98, doi:10.1175/JHM-D-14-0187.1, 2016.
- Mohanty, B. and Skaggs, T.: Spatio-temporal evolution and time-stable characteristics of soil moisture within remote sensing footprints with varying soil, slope, and vegetation, *Adv. Water Resour.*, 24, 1051–1067, doi:10.1016/S0309-1708(01)00034-3, 2001.
- Nash, J. E. and Sutcliffe, J. V.: River flow forecasting through conceptual models, I. A discussion of principles, *J. Hydrol.*, 10, 282–290, 1970.
- Nijssen, B., O'Donnell, G., and Lettenmaier, D.: Predicting the Discharge of Global Rivers, *J. Climate*, 14, 3307–3323, doi:10.1175/1520-0442(2001)014<3307:PTDOGR>2.0.CO;2, 2001.
- Rakovec, O., Hill, M. C., Clark, M. P., Weerts, A. H., Teuling, A. J., and Uijlenhoet, R.: Distributed Evaluation of Local Sensitivity Analysis (DELSA), with application to hydrologic models, *Water Resour. Res.*, 50, 409–426, doi:10.1002/2013WR014063, 2014.
- Rebetz, M., Mayer, H., Dupont, O., Schindler, D., Gartner, K., Kropp, J., and Menzel, A.: Heat and drought 2003 in Europe: a climate synthesis, *Annu. Forest. Sci.*, 63, 569–577, doi:10.1051/forest:2006043, 2006.
- Rosero, E., Yang, Z., Wagener, T., Gulden, L., Yatheendradas, S., and Niu, G.: Quantifying parameter sensitivity, interaction, and transferability in hydrologically enhanced versions of the Noah land surface model over transition zones during the warm season, *J. Geophys. Res.*, 115, D03106, doi:10.1029/2009JD012035, 2010.
- Samaniego, L., Kumar, R., and Attinger, S.: Multiscale parameter regionalization of a grid-based hydrologic model at the mesoscale, *Water Resour. Res.*, 46, W05523, doi:10.1029/2008WR007327, 2010.
- Schmocker-Fackel, P. and Naef, F.: More frequent flooding? Changes in flood frequency in Switzerland since 1850, *J. Hydrol.*, 381, 1–8, doi:10.1016/j.jhydrol.2009.09.022, 2010.
- Seneviratne, S. I., Lehner, I., Gurtz, J., Teuling, A. J., Lang, H., Moser, U., Grebner, D., Menzel, L., Schrott, K., Vitvar, T., and Zappa, M.: Swiss prealpine Rietholzbach research catchment and lysimeter: 32 year time series and 2003 drought event, *Water Resour. Res.*, 48, W06526, doi:10.1029/2011WR011749, 2012.
- Shrestha, P., Sulis, M., Simmer, C., and Kollet, S.: Impacts of grid resolution on surface energy fluxes simulated with an integrated surface-groundwater flow model, *Hydrol. Earth Syst. Sci.*, 19, 4317–4326, doi:10.5194/hess-19-4317-2015, 2015.

- Sood, A. and Smakhtin, V.: Global hydrological models: a review, *Hydrolog. Sci. J.*, 60, 549–565, doi:10.1080/02626667.2014.950580, 2015.
- Sulis, M., Paniconi, C., and Camporese, M.: Impact of grid resolution on the integrated and distributed response of a coupled surface-subsurface hydrological model for the des Anglais catchment, Quebec, *Hydrol. Process.*, 25, 1853–1865, doi:10.1002/hyp.7941, 2011.
- Sutanudjaja, E., van Beek, L., de Jong, S., van Geer, F., and Bierkens, M.: Calibrating a large-extent high-resolution coupled groundwater-land surface model using soil moisture and discharge data, *Water Resour. Res.*, 50, 687–705, doi:10.1002/2013WR013807, 2014.
- Teuling, A. J., Lehner, I., Kirchner, J. W., and Seneviratne, S. I.: Catchments as simple dynamical systems: Experience from a Swiss prealpine catchment, *Water Resour. Res.*, 46, W10502, doi:10.1029/2009WR008777, 2010.
- Todini, E.: Hydrological Catchment Modelling: Past, Present and Future, *Hydrol. Earth Syst. Sci.*, 11, 468–482, doi:10.5194/hess-11-468-2007, 2007.
- Troy, T. J., Wood, E. F., and Sheffield, J.: An efficient calibration method for continental-scale land surface modeling, *Water Resour. Res.*, 44, W09411, doi:10.1029/2007WR006513, 2008.
- Van Vliet, M. T. H., Yearsly, J. R., Ludwig, F., Vögele, S., Lettenmaier, D. P., and Kabat, P.: Vulnerability of US and European electricity supply to climate change, *Nature Clim. Change*, 2, 676–681, doi:10.1038/nclimate1546, 2012.
- Viviroli, D., Zappa, M., Gurtz, J., and Weingartner, R.: An introduction to the hydrological modelling system PREVAH and its pre- and post-processing-tools, *Environ. Model. Softw.*, 24, 1209–1222, doi:10.1016/j.envsoft.2009.04.001, 2009a.
- Viviroli, D., Zappa, M., Schwanbeck, J., Gurtz, J., and Weingartner, R.: Continuous simulation for flood estimation in ungauged mesoscale catchments of Switzerland – Part I: Modelling framework and calibration results, *J. Hydrol.*, 377, 191–207, doi:10.1016/j.jhydrol.2009.08.023, 2009b.
- Vivoni, E., Ivanov, V., Bras, R., and Entekhabi, D.: On the effects of triangulated terrain resolution on distributed hydrologic model response, *Hydrol. Process.*, 19, 2101–2122, doi:10.1002/hyp.5671, 2005.
- Vor`echovský, M.: Hierarchical refinement of latin hypercube samples, *Comput.-Aid. Civ. Infrastruct. Eng.*, 30, 394–411, doi:10.1111/mice.12088, 2015.
- Vor`echovský, M. and Novák, D.: Correlation control in small-sample Monte Carlo type simulations I: A simulated annealing approach, *Probabil. Eng. Mech.*, 24, 452–462, doi:10.1016/j.probengmech.2009.01.004, 2009.
- Vörösmarty, C., Moore III, B., Grace, A., and Gildea, M.: Continental scale models of water balance and fluvial transport: an application to South-America, *GlobAL Biogeochem. Cy.*, 3, 241–265, doi:10.1029/GB003i003p00241, 1989.
- Wada, Y. and Bierkens, M.: Sustainability of global water use: past reconstruction and future projections, *Environ. Res. Lett.*, 9, 104003, doi:10.1088/1748-9326/9/10/104003, 2014.
- Wagener, T. and Wheater, H. S.: Parameter estimation and regionalization for continuous rainfall-runoff models including uncertainty, *J. Hydrol.*, 320, 132–154, doi:10.1016/j.jhydrol.2005.07.015, 2006.
- Wang, Y., He, B., and Takase, K.: Effects of temporal resolution on hydrological model parameters and its impact on prediction of river discharge, *Hydrolog. Sci. J.*, 54, 886–898, doi:10.1623/hysj.54.5.886, 2009.
- Wen, Z., Liang, X., and Yang, S.: A new multiscale routing framework and its evaluation for land surface modeling applications, *Water Resour. Res.*, 48, W08528, doi:10.1029/2011WR011337, 2012.
- Wenger, S., Luce, C., Hamlet, A., Isaak, D., and Neville, H.: Macroscale hydrologic modeling of ecologically relevant flow metrics, *Water Resour. Res.*, 46, W09513, doi:10.1029/2009WR008839, 2010.
- Western, A., Zhou, S., Grayson, R., McMahon, T., Blöschl, G., and Wilson, D.: Spatial correlation of soil moisture in small catchments and its relationship to dominant spatial hydrological processes, *J. Hydrol.*, 286, 113–134, doi:10.1016/j.jhydrol.2003.09.014, 2004.
- Wood, E., Roundy, J., Troy, T., van Beek, L., Bierkens, M. P., Blyth, E., de Roo, A., Döll, P., Ek, M., Famiglietti, J., Gochis, D., van de Giesen, N., Houser, P., Jaffé, P., Kollet, S., Lehner, B., Lettenmaier, D., Peters-Lidard, C., Sivapalan, M., Sheffield, J., Wade, A., and Whitehead, P.: Hyperresolution global land surface modeling: Meeting a grand challenge for monitoring Earth’s terrestrial water, *Water Resour. Res.*, 47, W05301, doi:10.1029/2010WR010090, 2011.
- Yang, J., Reichert, P., and Abbaspour, K.: Bayesian uncertainty analysis in distributed hydrologic modeling: A case study in the Thur River basin (Switzerland), *Water Resour. Res.*, 43, W10401, doi:10.1029/2006WR005497, 2007.
- Zappa, M.: Multiple-Response Verification of a Distributed Hydrological Model at Different Spatial Scales, in: chap. 4. The sensitivity of distributed hydrological simulations to the spatial resolution of physiographic data, *ETH Zürich*, 35–51, 14895, doi:10.3929/ethz-a-004529728, 2002.
- Zappa, M. and Kan, C.: Extreme heat and runoff extremes in the Swiss Alps, *Nat. Hazards Earth Syst. Sci.*, 7, 375–389, doi:10.5194/nhess-7-375-2007, 2007.
- Zhao, R., Zuang, Y., Fang, L., Liu, X., and Zhang, Q.: The Xinanjiang model, *Hydrological forecasting – Prévisions hydrologiques*, Proceedings of the Oxford Symposium, April 1980, 129, 351–356, http://hydrologie.org/redbooks/a129/iahs_129_0351.pdf (last access: 7 August 2014), 1980.